A 3-d TWO-FLUID MODEL OF THE PLASMA VORTEX IN FRONT OF LH GRILLS

V. Petržílka, V. Fuchs, R. Klíma, L. Krlín, P. Pavlo, R. Pánek and F. Žáček
Association Euratom/IPP.CR, Prague, Czech Republic
M. Goniche and J. Gunn
Association Euratom/CEA Cadarache, France
D. Tskhakaya and S. Kuhn
Association Euratom/OeAW, Innsbruck, Austria

The term plasma vortex is an expression used for a rather complicated configuration of plasma flows, plasma density variations and electrostatic fields, which arise in front of an active lower hybrid (LH) grill in tokamaks. We have performed a two-fluid analysis of the plasma vortex, which arises because of local generation of fast electrons by LH waves in a thin layer just in front of the grill mouth [1,2]: As the electrons are pushed away from the grill mouth along the magnetostatic field lines, they leave the heavier ions behind, and thus an electrostatic field and consequent plasma flows are generated. Without the presence of spontaneously generated fields in front of the grill, this acceleration is limited to a narrow layer in front of the grill mouth, where higher LH harmonics can propagate. However, the electron acceleration and the radial width of the acceleration layer may be significantly enhanced by random fields, which are spontaneously generated near the antenna. By using test particle simulations of electron acceleration and its enhancement by random field effects for parameters relevant to conditions of the Tore Supra and Castor LH grills, it is possible to determine an effective potential W, which expels and accelerates the electron fluid [3]; the heavy ion fluid is then left in front of the grill mouth.

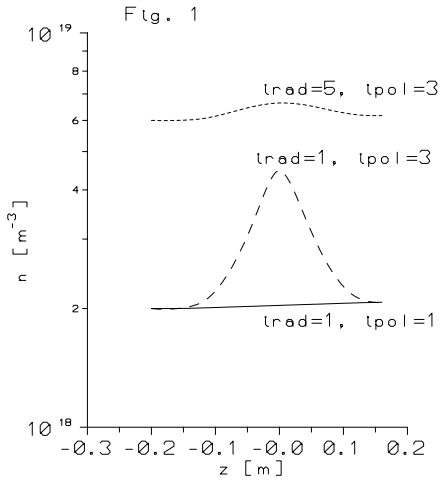

Profiles of the plasma density in front of the grill mouth.

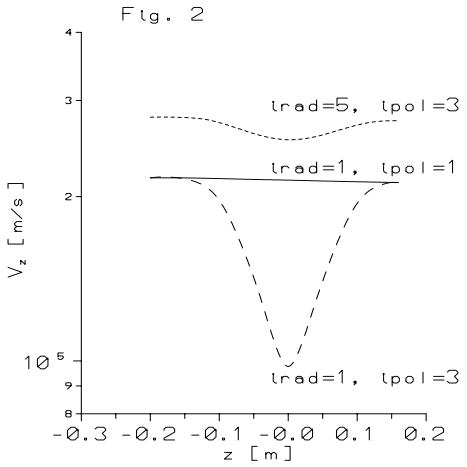

Profiles of the toroidal plasma velocity in front of the grill mouth.

It is useful to note that the value of W is much larger than the value of the well-known ponderomotive potential of the gradient ponderomotive forces in front of the grill. Consequently, and in particular at enhanced acceleration due to the presence of the random fields, a strong stationary toroidal z-directed electrostatic field arises, which is able to accelerate ions. The potential U of this electrostatic field varies also along the radial coordinate x and along the poloidal coordinate y. Therefore, also strong radial and poloidal electrostatic fields appear in front of the grill mouth.

As our previous 1-d and 2-d particle-in-cell (PIC) simulations [4, 5] of the plasma vortex were very time consuming because of the large region, which has to be modeled, we have now concentrated on two-fluid modeling. We prepared a first version of a 3-d two-fluid numerical model of a plasma vortex. We also obtained first results for the 3-d vortex configurations in front of an active grill mouth. This first version of the 3-d code computes plasma flows and electrostatic fields according to the following algorithm: It is assumed that the dominant physical process is the force equilibrium along the z-coordinate, and that the z-flows originate dominantly from the momentum balance in the z-direction. The equilibrium along the z-coordinate is described by the following equations (the electrom inertia is neglected):

$$0 = -enE_z - n\partial W(x,y,z)/\partial z - \partial p_e/\partial z \,, \qquad (1)$$

$$MnV_z\partial V_z/\partial z = neE_z - \partial p_i/\partial z - MSV_z \,, \qquad (2)$$

where M is the ion mass, V_z is the ion fluid velocity, the other notation is standard. For the source term S, we assume that $S = D_\perp n/(\lambda_n)^2 + S_i = C\, D_\perp n/(\lambda_n)^2$, where the term S_i and/or the value of C represent ionization. By adding Eqs. (1) and (2), we obtain,

$$V_z\partial V_z/\partial z = -(1/M)\partial W/\partial z - (c_s)^2\,(\partial n/\partial z)/n - SV_z/n \,, \qquad (3)$$

where c_s is the sound velocity. The equation continuity is also needed,

$$\partial(nV_z)/\partial z = S. \qquad (4)$$

In the above equations, we neglected terms proportional to the radial $\partial/\partial x$ and poloidal $\partial/\partial y$ derivatives, and to radial and poloidal plasma flow velocities, according to assumptions formulated above. The model expelling ponderomotive potential W in front of the grill was specified as

$$W = AM(c_s)^2\,[1 + \cos(2\pi z/L_g)]\,\sin(\pi y/L_{pol})\,\exp(-x/L_{rf}) \,, \qquad (5)$$

where L_g and L_{pol} denote the toroidal and poloidal dimensions of the grill waveguide row, and L_{rf} denote the radial scale length of the electron acceleration decrease into the plasma interior. For the unperturbed plasma density and temperature, we choose step and ramp profiles, $n = n_0\,(1+x/\lambda_n)$, $T_{e,i} = T_{e,i0}(1 + x/L_T)$. After computing the parallel flows and corresponding plasma density perturbations, the electrostatic field potential U(x,y,z) is computed by integration of E_z over z in all points of the x, y mesh, and the E_x and E_y

components are computed as corresponding derivatives of U(x,y,z). In the last step, the radial V_x and poloidal V_y velocities are computed as the drift velocities. Because of the above described simplified algorithm used in the computations, the results are fully valid only for plasmas exhibiting rather fast toroidal rotation. Typical results of the computations are shown in Figures 1 – 4, for A = 2, for C = 1.2, i.e. the source is slightly larger than radial transport, and for other parameters (with the exception of the large toroidal rotation velocity) close to the Tore Supra parameters: $n_0 = 2x10^{18}cm^{-3}$, $T_{e,i0} = 25$ eV, $D_\perp = 10$ m^2/s at the boundary, $\lambda_n =$ 1 cm, $L_T = 3$ cm, $L_g = 30$ cm, $L_{pol} = 10$ cm, $L_{rf} = 2$ cm. The large unperturbed initial rotation velocity of the order of c_s might occur in beam heated plasmas. Let us also note that the results are not too sensitive to variations of C.

The results presented in the figures show the z-profiles at five points of the x (irad = 1,…,5) and y (ipol = 1,…,5) mesh. The value irad = 1 corresponds to x = 0 just at the grill mouth, while irad = 5 corresponds to the radial distance of x = 2 cm from the grill mouth. The remaining values irad = 2, 3, 4 then correspond to x = 0.5, 1, 1.5 cm, respectively. Similarly, ipol = 1 corresponds to the value of the poloidal coordinate y = 0 at the grill row boundary (poloidally), the value ipol = 5 corresponds to the other poloidal boundary of the row (to y = 10 cm in our model computations). The values ipol = 2, 3, 4 then correspond to y = 2.5, 5, 7.5 cm, respectively.

Fig. 3

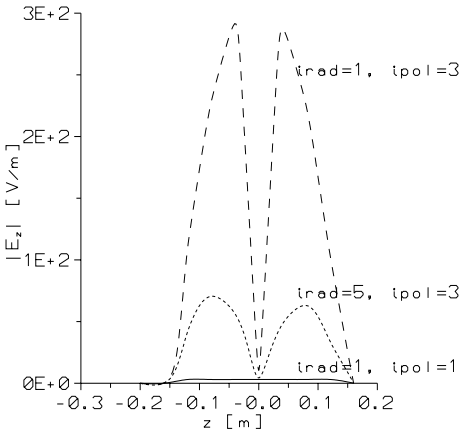

Profiles of the absolute value of the toroidal component of the electrostatic charge separation field.

Fig. 4

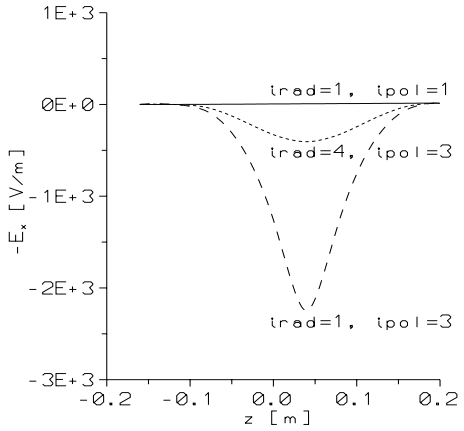

Profiles of the radial component of the charge separation electrostatic field in front of the grill mouth.

Let us comment some specific features of the results. We can see in Fig. 1 how the plasma density grows near z = 0, in particular radially just at the grill mouth and at the poloidal maximum of the rf field amplitude, i.e., for irad = 1 and ipol = 3. This growth is related to the decrease of the toroidal plasma flow velocity at the same place, cf. Fig. 2. This decrease in the flow velocity is due to the slowing down of the electron component by the expelling force of the rf field in the left half of the grill for $z < 0$. By the toroidally directed component of the charge separation electrostatic field, the ions are also decelerated for $z < 0$, and the flow

velocity decreases. The absolute value profiles of the E_z charge separation field are shown in Fig. 3. Let us note that the dashed lines in the left half of the grill (for $z < 0$) correspond to negative values of the toroidal z- component of the electrostatic field. Profiles of the radial component E_x of the electrostatic field are shown in Figure 4. Let us only note that the maximum value of the poloidal E_y field is about 500 V/m, and that the maximum values of the radial and poloidal flow velocities are then about several hundreds meters per second.

The plasma density growth shown in Figure 1 will result in changes in the wave coupling (in variations of the reflection coefficient) and in growth of the energy carried by the accelerated electrons, because of the larger number of accelerated electrons in a higher density plasma. This plasma density growth would in turn further amplify the intensity of the vortex. The plasma density growth might result also in a change of the launched LH wave spectrum. For a higher unperturbed rotation velocity, the density growth would be less emphasized, and the selfconsistent amplification of the vortex would be lower. Let us note that for a zero unperturbed rotation velocity, a density decrease [4, 5] was obtained.

For larger values of the tilt of the magnetostatic field, the density growth would not be limited to the region around $z = 0$, but it would acquire the form of a toroidally oriented "sausage" along the poloidal plane of symmetry (ipol = 3) of the grill row. This would mean that the consequences of the density growth would be more significant in a larger area in front of the grill mouth. Corresponding computations are envisaged in a continuation of this study.

In conclusion, we have found that the acceleration of electrons in front of the LH grill mouth by the field of the LH wave results in significant growth in plasma density in front of the grill, which should lead to ensuing further amplification of the vortex, and to changes in the launched LH wave spectrum. The density variation is sensitive to the value of the unperturbed plasma toroidal plasma velocity in front of the grill, and apparently also to the tilt of the magnetostatic field in front of the grill.

Acknowledgments: This work was partly supported by the Czech Grant GACR 202/00/1217. One of the authors (D. Tskh.) acknowledges partial support from Austrian Research Funds (FWF) project P12477-TPH.

References:

[1] M. Goniche et al., Nuclear Fusion 38 (1998) 919.
[2] K.M. Rantamaki et al., Phys Plasmas 5 (1998) 2553.
[3] V. Petržílka et al., 18th IAEA Fusion Energy Conference, Sorrento, Italy, October 4-10, 2000, paper CN-77/EXP4/07, Book of Abstracts p. 42.
[4] F. Žáček et al., 27th EPS Conference on Plasma Physics and Controlled Fusion, Budapest, Hungary, June 12-16, 2000, Book of Abstracts p. 349.
[5] D. Tskhakaya et al., 27th EPS Conference on Plasma Physics and Controlled Fusion, Budapest, Hungary, June 12-16, 2000, Book of Abstracts p. 107.